An Electrochemical Quartz Crystal Impedance Study on the Rising of an Aqueous Solution Meniscus for a Partially Immersed Gold Electrode during the Electrochemical Reduction of Oxygen

Qingji XIE,† Youyu ZHANG, Xiaoming XIAO, Yanghui GUO, Xiangjun WANG, and Shouzhuo YAO

Chemical Research Institute, Hunan Normal University, Changsha 410081, P. R. China

An electrochemical quartz crystal impedance system (EQCIS) was used to study the resonance behavior of an AT-cut 9-MHz piezoelectric quartz crystal (PQC) with its Au electrode partially immersed in KCl, Na_2SO_4 and $NaClO_4$ aqueous solutions, respectively. An *in situ* determination of the immersed area and the height of the electrode was achieved by simultaneous measurements of the PQC electroacoustic admittance and the electrochemical impedance. The rising of the solution meniscus for a gold electrode partially immersed in aqueous solutions was found at oxygen reduction potentials and evaluated *versus* the electrolyte, electrolyte concentration, solution pH and oxygen concentration. The solution meniscus rising was explained based on a lowering of the contact-angle hysteresis and a continued collection of the water product at the solid-gas-solution interface during oxygen reduction.

(Received August 9, 2000; Accepted October 19, 2000)

The electrochemical quartz crystal impedance system (EQCIS), which allows simultaneous and fast measurements of the piezoelectric quartz crystal (PQC) electroacoustic impedance during electrochemical perturbations, provides multidimensional piezoelectric information *in situ* in electrochemical processes.[1–10] The PQC impedance has been analyzed based on a Butterworth–Van Dyke (BVD) equivalent electrical circuit composed of a motional arm and a static arm in parallel. The motional arm contains three equivalent-circuit elements in series, namely, the motional resistance (R_1), the motional inductance (L_1), and the motional capacitance (C_1), while the static arm contains only the static capacitance (C_0; note that the parasitic capacitance between the two PQC electrodes is also included in C_0 in an experiment). The equivalent-circuit parameters have distinct physical meanings and can be obtained by fitting the experimental data of the conductance (G) and susceptance (B) *versus* the frequency (f) to the BVD model.[1–12] Besides the four independent equivalent-circuit parameters, three characteristic frequencies of the PQC resonance have been used frequently,[8] namely, the resonant frequency (f_0) at which the reactance (X) and susceptance (B) of the motional arm vanish ($f_0 = 1/[2\pi(L_1C_1)^{1/2}]$); also, the series resonant frequency (f_s) and the parallel resonant frequency (f_p), which are the lower frequency and the higher frequency, where the X and B of the BVD circuit vanish, and are dependent on all four equivalent-circuit parameters, according to our derivations.[10]

Compared with the conventional electrochemical quartz crystal microbalance (EQCM) that generally records the piezoelectric information only on the PQC oscillation frequency, the EQCIS can provide direct insight into foreign film rigidity,[1–10] which is very important for the PQC sensor to be used for the determination of the foreign film mass *via* the resonant frequency shift and the Sauerbrey equation (*i.e.* its microbalance application). The shape of the electroacoustic admittance curve of the PQC measured by this sophisticated technique can be a characteristic of the film viscoelastic properties, *i.e.* the deposition of a viscous film decreases the peak height of the conductance (G) curve and increases its half peak width ($\Delta f_{G1/2}$) and the motional resistance (R_1), though the peak height and width change little after depositing a rigid film (*e.g.* metal deposition) onto the PQC electrode surface.[4,7,8] A slight increase in R_1 ($\Delta f_0/\Delta R_1 \approx -300$ Hz Ω^{-1}) during the deposition of silver onto gold in a 2.0 mmol l^{-1} $AgNO_3$ + 0.20 mol l^{-1} $HClO_4$ aqueous solution has been ascribed to an increase in the electrode surface roughness due to the introduction of silver particle deposits, leading to an increase in the friction force against the PQC oscillation, and thus R_1.[7,8,12] If $\Delta f_{G1/2}$ is defined as the frequency difference of the two frequency points at the half peak height in the G spectrum, and it is realized that the conductance at the half peak height is $G = G_{max}/2 = 1/(2R_1)$, combining it with the G equation given by the BVD circuit gives[8]

$$f_{LG1/2} = f_{Bmax} = (-R_1C_1 + \sqrt{R_1^2C_1^2 + 4L_1C_1})/(4\pi L_1C_1), \quad (1)$$

$$f_{HG1/2} = f_{Bmin} = (R_1C_1 + \sqrt{R_1^2C_1^2 + 4L_1C_1})/(4\pi L_1C_1), \quad (2)$$

$$\Delta f_{G1/2} = f_{HG1/2} - f_{LG1/2} = f_{Bmin} - f_{Bmax} = R_1/(2\pi L_1), \quad (3)$$

where $f_{HG1/2}$ and $f_{LG1/2}$ are the higher and lower frequencies at the half peak height in the G spectrum, and f_{Bmin} and f_{Bmax} are the frequencies at the minimum and maximum B values, respectively; all symbols are in their international units.

The piezoelectric quartz crystal was first developed as a mass sensor in the gaseous phase; and its utilization in the liquid phase began about 20 years ago.[1] To the best of our knowledge,

† To whom correspondence should be addressed.
E-mail: xieqj@pubic.cs.hn.cn

researchers have paid little attention so far to the responses of equivalent-circuit parameters to the immersed electrode area and/or height of a partially immersed PQC sensor, although investigations concerning the partial immersion of a PQC is important for better understanding the liquid loading effect on the resonance behavior of the widely-used submerged PQC sensors and for applying the PQC as a sensitive solution height sensor. In addition, partially immersed PQC electrodes may also be helpful for investigating the electrochemical oxidation of hydrogen or the reduction of oxygen present in the surrounding environment, and thus for better understanding the working mechanism of gas-diffusion electrodes.[13-15] In this work, we hence examined the effects of the immersed electrode height and area on the equivalent-circuit parameters using an EQCIS; by using the PQC sensor as an immersion position indicator, the rising of the aqueous solution meniscus during oxygen reduction was found and is discussed in detail.

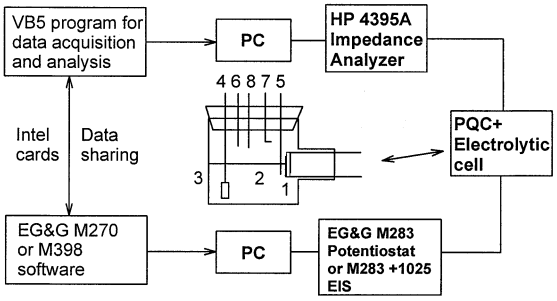

Fig. 1 Schematic representation of the EQCIS used in this work. 1, PQC sealed on one terminal of a glass tube using silica rubber adhesive; 2, test solution; 3, glass electrolytic cell; 4, counter electrode; 5, reference electrode with a supporting electrolyte salt bridge; 6, solution inlet (the solution was added to the electrolytic cell along the cell wall); 7, nitrogen (or oxygen) inlet when needed; 8, nitrogen (or oxygen) outlet when needed.

Experimental

Instrumentation and reagents

The EQCIS used is described in Fig. 1, which allowed fast and simultaneous measurements of the PQC impedance *via* an HP 4395A impedance analyzer and the electrochemical impedance *via* an EG&G M283 + 1025 electrochemical impedance system (EIS)[10] (or dc electrochemical signals with the EG&G M283 potentiostat alone).[7-9] The conductance (G) and susceptance (B) of the PQC resonance were measured synchronously on the HP 4395A equipped with an HP 43961A impedance test adapter and an HP 16092A test fixture. A program was written in Visual Basic (VB) 5.0 to control the HP 4395A and to acquire admittance data *via* an HP 82341C high-performance HP-IB interface card for Windows 3.1/NT/95. Admittance measurements were conducted under conditions of 201 points, a frequency span of 40 kHz covering the resonant frequency of the PQC, IF BW of 10 kHz and a source power of 0.5 dB m. Real-time analyses of the acquired admittance data were achieved in the same VB 5.0 program by fitting each group of G and B data to the BVD model based on the Gauss–Newton nonlinear least-squares fitting algorithm. We only selected 51 groups of G and B *versus* frequency data from the 201 groups of experimental data for the non-linear fitting here, and the center frequency of the 51 groups of data was always the frequency giving the maximum G value (G_{max}). This method, namely, the frequency-point-selection fitting routine, can save fitting time and reduce errors resulting from the time hysteresis during recording one G or B spectrum,[8] since 0.22 s was experimentally required for the HP4395A to complete a sweep of all 201 frequency points, but only 55 ms was needed for the 51 frequency points selected. R_1, C_0, f_0 and $1/C_1$ were generally chosen as estimation parameters during the fitting.[7-10] The frequency giving the G_{max} value was automatically found by the fitting program and used as the initial value of f_0 as well as the center frequency of the 51 frequency points chosen, while $1/G_{max}$ was automatically used as the initial value of R_1. Hence, only initial values of $1/C_1$ and C_0 were required to be roughly given before the fitting. Equivalent-circuit parameters were obtained at a time interval of ~1.6 s and displayed continuously during admittance measurements when the sum and the relative sum of residual squares had become minimum.[8,10] The VB program is available from the authors upon request. AT-cut 9-MHz piezoelectric quartz crystals (1.25 cm in diameter) were used here. A gold electrode of 0.70-cm diameter on one side of the PQC, vacuum-evaporated by using an Eiko IB-3 ion coater and a highly pure gold foil purchased from Hitachi Inc., was in contact with the solution, and served as the working electrode, while a silver electrode on the other side of the PQC was located in air. The gold electrode had a surface polished to ~0.1 μm, as examined by SEM. To remove possible surface contamination, the gold electrode surfaces were generally treated with H_2SO_4 + H_2O_2 (v/v 3:1) for 5 min and then rinsed thoroughly with water. A saturated KCl calomel electrode (SCE) with a supporting electrolyte salt bridge served as a reference, and all potentials in this work were referenced to it. A glassy carbon plate served as the counter electrode. A glass three-electrode electrolytic cell was used. A 50-ml burette was used to gradually add the test solution to the electrolytic cell, and the PQC Au electrode was perpendicular to the bulk solution surface. Doubly distilled water and freshly prepared solutions were used throughout. The contact angles were measured using a JJC-II contact angle measurement instrument (Changchun Fifth Optical Instruments Factory, China). The 1-dodecanethiol-modified gold electrode used in this work was achieved by dipping a PQC gold electrode in an acetone solution containing 5 mmol l^{-1} 1-dodecanethiol for 6 h, and the contact angle for water was 101° after the thiol modification. All experiments were carried out at 10 ± 1°C.

Procedures

Prior to the PQC admittance measurements, the HP 43961A impedance test adapter and the HP 16092A test fixture were calibrated and compensated using HP standard impedance kits. During experiments of gradual immersion of the PQC gold electrode, the test solution was gradually added from the burette until submergence of the PQC; the PQC impedance and the electrochemical impedance (EI) were measured simultaneously. The EI was measured at 3 kHz, 5 mV rms and an open-circuit potential. The EI measurement frequency was sufficiently high that the electrochemical interface could be simplified as a circuit of R_e in series with C_d,[10,16,17] where R_e denotes the electrolyte solution resistance, and C_d is the double-layer capacitance. For cyclic voltammetric and potential-step experiments, a certain volume of test solution was added to immerse the Au electrode to a specific position, and after the equivalent-circuit parameters became relatively stable, electrochemical perturbations were then applied during measurement of the PQC impedance.

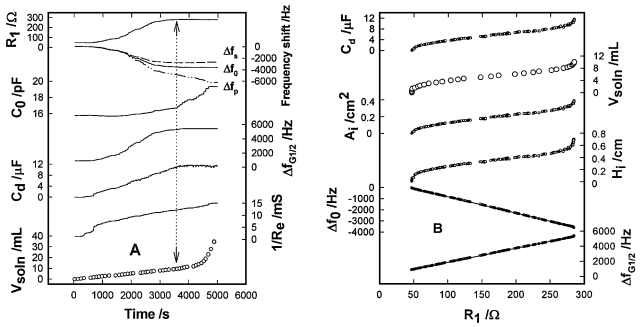

Fig. 2 EQCIS responses as functions of time (A) and C_d, V_{soln}, the immersed electrode area (A_i), the immersed electrode height (H_i), Δf_0 and $\Delta f_{G1/2}$ as functions of R_1 (B) during the addition of 0.20 mol l^{-1} KCl aqueous solution. The lower edge of the circular Au electrode touched the solution at time zero, and the electrode was totally immersed at the time indicated by the arrows. Electrochemical impedance measurements were conducted at 3 kHz, 5 mV rms and an open-circuit potential.

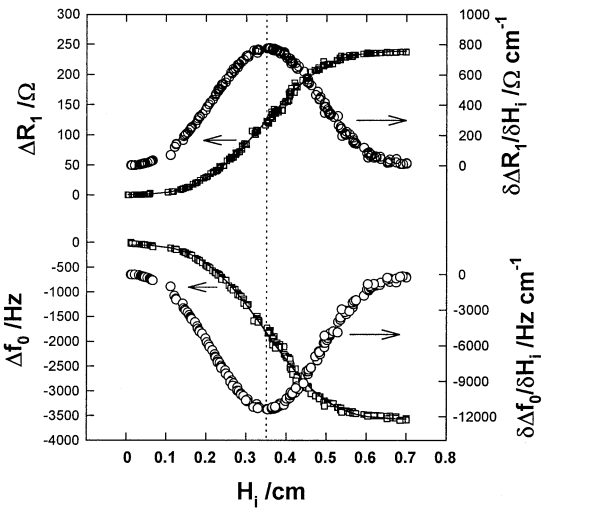

Fig. 3 ΔR_1, Δf_0, $\delta\Delta R_1/\delta H_i$ and $\delta\Delta f_0/\delta H_i$ as functions of the immersed electrode height (H_i) for the experiment shown in Fig. 2. The dashed line indicates the electrode center position. The solid lines show fitted results of ΔR_1 and Δf_0 according to Eq. (5).

Results and Discussion

Responses of equivalent-circuit parameters to partial immersion of a PQC electrode

Figure 2 shows the experimental results of simultaneous measurements of the PQC impedance and the electrochemical impedance during gradual immersion of the PQC by the addition of a 0.20 mol l^{-1} KCl aqueous solution with the burette. As expected, along with an increase in the added solution volume (V_{soln}) until submergence of the PQC Au electrode, $\Delta f_{G1/2}$ (calculated from Eq. (3)), R_1 and C_0 increased, and f_0, f_s and f_p decreased. The sensitivities of the three frequencies followed the sequence $-\Delta f_p > -\Delta f_0 > -\Delta f_s$, although theoretically and experimentally one always obtains $f_p > f_s > f_0$.[10] C_0 increased notably even after the Au electrode was totally immersed, indicating an increase in the parasitic capacitance due to the dielectric connection between the two PQC electrodes *via* the solution and the silica rubber adhesive used for sealing the PQC electrodes.

By considering that L_1 of the 9-MHz PQC changes little from air to an aqueous solution environment (<3% change),[7] the following equation reflecting liquid loading effects can be obtained from Martin's equations[8-11] and Eq. (3):

$$2\pi L_q \delta\Delta f_{G1/2L} \approx \Delta R_L = 2\pi f \Delta L_L = -4\pi L_q \Delta f_{0L} \sqrt{f\mu_q} / \sqrt{\bar{c}_{66} f_{0g}} \approx -4\pi L_q \Delta f_{0L}, \quad (4)$$

where $\delta\Delta f_{G1/2L}$, Δf_{0L}, ΔR_L and ΔL_L are the changes in $\Delta f_{G1/2}$, f_0, R_1 and L_1 due to variations of the solution density and viscosity, respectively, f_{0g} is the resonant frequency in air, ρ_q (2648 kg m^{-3}) and μ_q (2.947×10^{10} N m^{-2}) are the density of quartz and the shear modulus for the AT-cut quartz, respectively, L_q is the motional inductance for the PQC in air, and $\bar{c}_{66}$ (2.957×10^{10} N m^{-2}) is the lossy piezoelectrically stiffened quartz elastic constant.[2,7-11] The calculated slopes of Δf_{0L} and $\delta\Delta f_{G1/2L}$ *versus* ΔR_L are –9.39 and 18.78 Hz Ω^{-1} for the 9 MHz crystal used in this work, respectively, and one always obtains $\delta\Delta f_{G1/2L} \approx -2\Delta f_{0L}$ for various PQCs if the change in L_1 is small.

We found that Δf_0 and $\Delta f_{G1/2}$ were linearly related to R_1 with regression equations as $\Delta f_0 = -14.75R_1 + 659.6$ ($r = -0.9999$) and $\Delta f_{G1/2} = 18.59R_1 - 2.5$ ($r = 0.9999$); however, the slope of Δf_0 *versus* R_1, –14.75 Hz Ω^{-1} deviates notably from the value of –9.39 Hz Ω^{-1} calculated from Eq. (4) (57% deviation), suggesting that Martin's model dealing with the liquid loading effect for submerged PQC electrodes[8-11] can not well explain the behavior of the partially immersed electrode here. We also examined the slope of Δf_0 *versus* R_1 for a submerged PQC electrode using a series of sucrose aqueous solutions; a slightly larger slope value of Δf_0 *versus* R_1 than that calculated from Martin's model could be obtained (11% deviation), which is in good agreement with previous reports,[9,18,19] and may be ascribed to the effects of surface roughness.[1,11] The deviation between the experimental and theoretical slopes of Δf_0 *versus* R_1 for a partially immersed PQC electrode is significantly larger than that for a submerged electrode, suggesting that, besides the effects of electrode surface roughness, other factors that are unclear at present should be effective.

Both $1/R_e$ and C_d increased with increasing the immersed electrode area, but C_d could reach a relatively stable value after total immersion of the PQC electrode, suggesting that C_d may be proportional to the immersed electrode area. Based on this assumption, we evaluated the relationship between the immersed electrode area (A_i) or height (H_i) and R_1 (or f_0 *etc.*), as shown in Figs. 2 and 3. Note that H_i was obtained digitally from the following equation for the circular Au electrode: $A_i = \pi r^2\theta/360 - r(r - H_i)\sin(\theta/2)$, where r (= 0.35 cm) is the electrode radius, θ is the arc angle (in degree) corresponding to the immersed part of the electrode and $\cos(\theta/2)=(r - H_i)/r$. As shown in Fig. 3, we found empirically that curves of Δf_0 and ΔR_1 *versus* H_i could be well simulated by sigmoidal Weibull curves with the following equation:

$$S = a - (a - b)e^{-(kH_i)^d}, \quad (5)$$

where S denotes ΔR_1 or Δf_0, and the four parameters (here all given in four figures) are, a = 239.4 Ω, b = 1.223 Ω, k = 2.558 cm^{-1} and d = 3.290 for ΔR_1; and a = –3571 Hz, b = –53.65 Hz, k = 2.553 cm^{-1} and d = 3.282 for Δf_0, respectively.

It is obvious from Fig. 3 that the response sensitivity of the PQC to the liquid loading is highest at the PQC electrode center, which is similar to the highest mass-sensitivity characteristic at

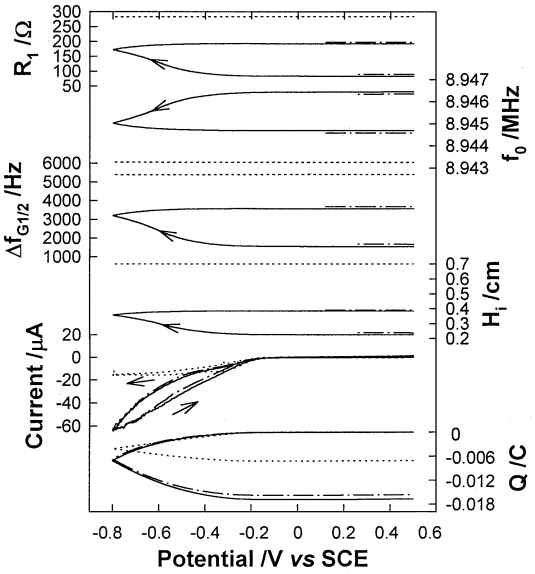

Fig. 4 EQCIS and H_i responses for a PQC Au electrode partially (solid and dotted lines) and totally (dashed lines) immersed in 0.20 mol l^{-1} KCl aqueous solution during potential cycling between 0.5 and –0.8 V *vs*. SCE. dE/dt = 2 mV s^{-1}. The solid and dashed lines: the quartz crystal impedance was measured simultaneously during the whole potential cycling; the dotted lines: the HP 4395A impedance analyzer was disconnected during potential cycling from 0.26 to –0.8 and then to 0.12 V *vs*. SCE. The solution was exposed to air.

the electrode center, as examined by Ward *et al*.[20,21] A $\delta\Delta R_1/\delta H_i$ value of ~800 Ω cm^{-1} was obtained at the center of the PQC Au electrode; a measurement resolution of H_i as high as ~4 μm near the electrode center can thus be estimated based on a triplication of the signal-to-noise ratio and a 0.1 Ω noise level of R_1. V_{soln} *vs*. R_1 is also plotted in Fig. 2B, and a similar sensitivity behavior can be seen. We found that H_i was linearly related to V_{soln} with a regression equation as $H_i = 0.067V_{soln} - 0.011$ (r = 0.9913). By considering that our electrolytic cell was designed with a uniform volume distribution in the PQC electrode region and a 10.2 ml volume of solution was experimentally required to immerse the Au electrode totally (0.70 cm electrode height), the slope of H_i *versus* the immersed electrode height estimated from V_{soln} was calculated to be 0.976, which is close to unity, suggesting that C_d is truly proportional to the immersed area; also, simultaneous measurements of the PQC impedance and the electrochemical impedance provide an effective method for an *in situ* determination of the immersed area and height of the electrode. Note that it seems to be difficult to take V_{soln} as a very accurate measure of H_i, because the effects of the contact-angle hysteresis[22-25] led to a slow and gradual rising of the solution meniscus experimentally for a specific value of V_{soln} (required ~30 min to achieve relatively stable responses of equivalent-circuit parameters).

Rising of an aqueous solution meniscus for a partially immersed gold electrode during oxygen reduction

Figure 4 shows the EQCIS and H_i responses to potential cycling from 0.5 to –0.8 and then to 0.5 V *vs*. SCE for an Au electrode partially or totally immersed in a 0.20 mol l^{-1} KCl aqueous solution. The EQCIS responses for the submerged PQC sensor were very small here; however, for a partially immersed Au electrode at oxygen reduction potentials, R_1 and $\Delta f_{G1/2}$ increased notably while f_0 decreased significantly, and f_0 and $\Delta f_{G1/2}$ were linearly related to R_1 with regression equations

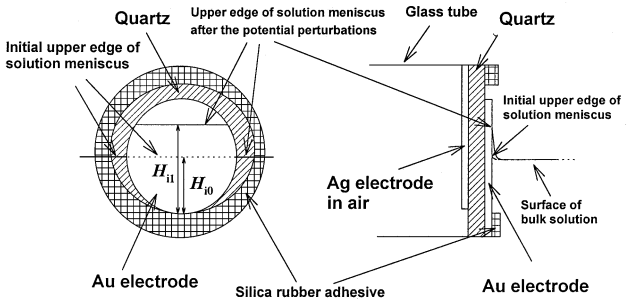

Fig. 5 Sketch map of the aqueous solution meniscus rising on the PQC Au electrode (not to scale). H_{i0} and H_{i1} are the immersed electrode height (H_i) before the potential perturbations and during or after the potential perturbations, respectively.

as $f_0 = -15.83R_1 + 8947745.8$ (r = –0.9998) and $\Delta f_{G1/2} = 18.49R_1 + 18.28$ (r = 1.0000). Significant changes in these parameters, which are similar to those found during the gradual immersion of the PQC Au electrode by the addition of a 0.20 mol l^{-1} KCl aqueous solution (Fig. 2), should suggest increases in the liquid loading to the partially immersed PQC Au electrode, *i.e*. the rising of the solution meniscus during potential cycling at the oxygen reduction potentials, as also clearly observed by the naked eye. Figure 5 shows a schematic drawing of the solution meniscus rising in experiments, note that the meniscus rising was observed on the Au electrode but not on the quartz surface, *i.e*. it was confined to the electrochemical reaction zone, suggesting that electrochemical reactions were essential for the meniscus rising. By using the H_i *vs*. R_1 data given in Eq. (5) and Figs. 2 and 3, the increase in the immersed electrode height at oxygen reduction potentials was estimated, as shown in Fig. 4, too. To evaluate the agitation effect of shear oscillation of the PQC in its resonance region on the solution meniscus rising, we also conducted an experiment when the PQC's oscillation did not occur *via* disconnecting the HP 4395A impedance analyzer at the oxygen reduction potentials. As shown in Fig. 4, the EQCIS and H_i responses for oscillating and non-oscillating PQC electrodes after potential cycling are quite comparable with each other, indicating that the agitation effect of the PQC's shear oscillation is negligible here, and that the rising of the solution meniscus can by no means be ascribed to the PQC oscillation. In addition, a current increase at the oxygen reduction potentials was seen for a partially immersed Au electrode, and the current during a reversal potential sweep was higher than that during the initial cathodic sweep at a potential between –0.8 and –0.25 V *vs*. SCE, also implying that the immersed electrode area and height had most likely been changed during the reversal positive-going potential sweep. The marked current increase on partially raising an electrode above the electrolyte was also found in the case of the oxygen reduction on copper, silver and nickel electrode sheets[15] and in the case of the hydrogen oxidation on platinum electrodes.[13,14] The effects of meniscus formation on the electrode current during hydrogen reduction when partially raising a platinum electrode above the electrolyte have been examined in detail both experimentally and theoretically,[13,14] showing that the slow diffusion of molecular hydrogen through the upper edge of the electrolyte meniscus and a thin liquid film above the intrinsic meniscus is the determining step of hydrogen oxidation, and that the reaction zone is confined to a narrow band close to the upper meniscus edge. However, to the best of our knowledge, the rising of the solution meniscus during oxygen reduction for partially

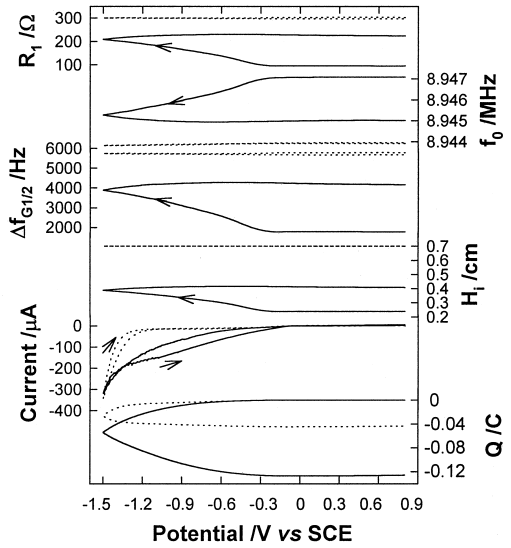

Fig. 6 EQCIS and H_i responses for a PQC Au electrode partially (solid lines) and totally (dashed lines) immersed in 0.10 mol l^{-1} Na_2SO_4 aqueous solution during potential cycling between 0.8 and –1.5 V *vs*. SCE. dE/dt = 2 mV s^{-1}. The solution was exposed to air.

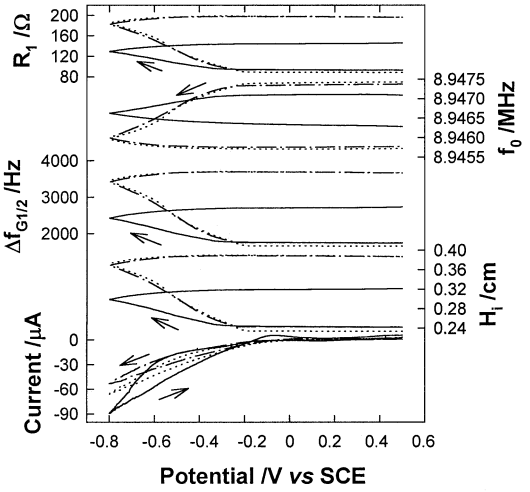

Fig. 7 EQCIS and H_i responses during potential cycling between 0.5 and –0.8 V *vs*. SCE for a PQC Au electrode partially immersed in 0.10 mol l^{-1} $NaClO_4$ + 0.10 mol l^{-1} NaOH (solid lines), 0.20 mol l^{-1} $NaClO_4$ + 1.0 mmol l^{-1} $HClO_4$ (dashed lines) and 0.20 mol l^{-1} $NaClO_4$ (dotted lines) aqueous solutions. dE/dt = 2 mV s^{-1}. The solutions were exposed to air.

immersed electrodes seems not to have been reported and examined so far; we thus conducted experiments as follows to clarify the mechanism responsible for this interesting phenomenon observed in this work.

Similar solution meniscus rising phenomena were also found in cyclic voltammetric experiments between 0.5 and –0.8 V *vs*. SCE at 2 mV s^{-1} conducted in Na_2SO_4 and $NaClO_4$ aqueous solutions; even the electrolyte concentration was reduced to 1 mmol l^{-1}, but a lower electrolyte concentration brought about a smaller EQCIS response. In addition, as shown in Fig. 6 for an Au electrode partially immersed in a 0.10 mol l^{-1} Na_2SO_4 aqueous solution, similar EQCIS responses were found even during potential cycling between 0.8 and –1.5 V *vs*. SCE where hydrogen evolution occurred significantly at potentials negative to –1.3 V *vs*. SCE. Figure 7 shows the effects of the solution pH on the EQCIS and H_i responses for a PQC Au electrode partially immersed in $NaClO_4$ solutions. We found that the R_1 and f_0 responses were comparable with each other in acidic and neutral $NaClO_4$ solutions, but were significantly larger than those in the alkaline solution. In addition, the potential of zero charge (PZC) for gold reported in acidic $NaClO_4$ aqueous solutions was between 0.1 and 0.18 V *vs*. SHE (*i.e*. from –0.15 to –0.07 V *vs*. SCE),[26] but the R_1 and f_0 responses between –0.2 and 0.2 V *vs*. SCE were very small (within ~1 Ω and ~10 Hz), indicating that the electrocapillary effect[27] on the rising of aqueous solution meniscus is very minor here. A cyclic voltammetric EQCIS experiment for an Au electrode partially immersed in 1.0 mmol l^{-1} $HClO_4$ aqueous solution also showed the same results.

To examine the effects of oxygen, we conducted experiments for an Au electrode partially immersed in an oxygen-treated (or nitrogen-treated) KCl aqueous solution in oxygen (or nitrogen) (the solution was saturated with oxygen or nitrogen for 30 min, and then added to the electrolytic cell that had been saturated with oxygen or nitrogen for 30 min, respectively), and found that the f_0, R_1 and $\Delta f_{G1/2}$ responses in oxygen were slightly higher than those shown in Fig. 4 for the same solution in air, but those in nitrogen were very small, as shown in Fig. 8. In addition, an experiment was conducted using a 1-dodecanethiol-modified PQC Au electrode partially immersed in a 0.20 mol l^{-1} KCl aqueous solution exposed to air (R_1 = 86 Ω), and the responses of the PQC impedance obtained during the potential cycling between 0.5 and –0.8 V *vs*. SCE at 2 mV s^{-1} were also very small (ΔR_1 < 2 Ω, Δf_0 < 20 Hz, $\delta\Delta f_{G1/2}$ < 30 Hz and ΔH_i < 40 μm). Simultaneously, the current observed at –0.8 V *vs*. SCE was only –2 μA, indicating that the 1-dodecanethiol self-assembled monolayer formed on the Au electrode effectively blocked the electrochemical reduction of oxygen. These experiments demonstrate that the presence of oxygen and its electrochemical reduction are both essential for the rising of solution meniscus. Therefore, we may conclude that the continued collection of the water produced by oxygen reduction occurred at the upper edge of the solution meniscus (Au-gas-solution interface), *i.e*. $O_2 + 4H^+ + 4e = 2H_2O$ for acidic and neutral solutions and $O_2 + 2H_2O + 4e = 4OH^-$ for alkaline solutions, is important for the rising of the aqueous solution meniscus on partially immersed electrodes. For the Au electrode partially immersed in 0.20 mol l^{-1} KCl, 0.10 mol l^{-1} Na_2SO_4 and 0.20 mol l^{-1} $NaClO_4$ aqueous solutions (pH ~6.5), respectively, the solution pH at the upper edge of the lifted solution meniscus became ~10.5, as measured immediately after potential perturbations using pH test papers, demonstrating that a reduction of oxygen had truly occurred in this zone, and that the electrode product collection explanation seems to be plausible for the rising phenomenon of aqueous solution meniscus observed for the partially immersed Au electrode. In addition, the current increase observed at partially immersed Au electrodes can be explained based on the two following facts: (1) more continuous and abundant supply of oxygen during its reduction, as the electrode was partially exposed to an air or oxygen atmosphere; (2) a pH increase at the upper edge of the solution meniscus during oxygen reduction, as larger currents of oxygen reduction were observed experimentally in the alkaline solution than in acidic and neutral solutions (Fig. 7).

Figure 9 shows cyclic voltammogramms for the Au electrode partially and totally immersed in solutions containing 2.00 mmol l^{-1} $K_4Fe(CN)_6$. It can be seen that the partially immersed Au electrode (curve 3, R_1 = 209 Ω) obtained after a potential

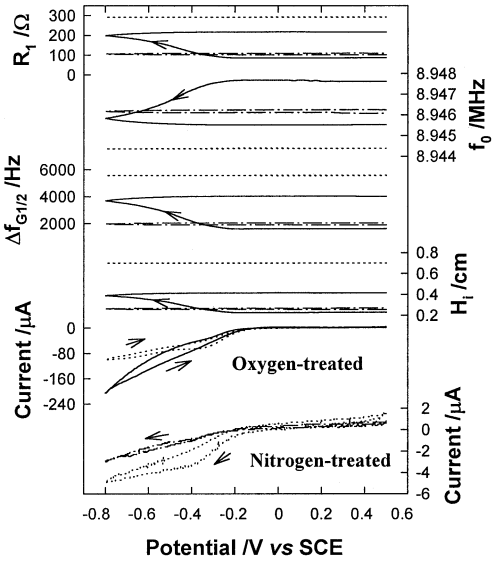

Fig. 8 EQCIS and H_i responses during potential cycling between 0.5 and –0.8 V *vs*. SCE for a PQC Au electrode partially (solid and dotted lines) and totally (dashed lines) immersed in 0.20 mol l^{-1} KCl aqueous solution treated with oxygen (solid lines) or nitrogen (dotted lines). dE/dt = 2 mV s^{-1}.

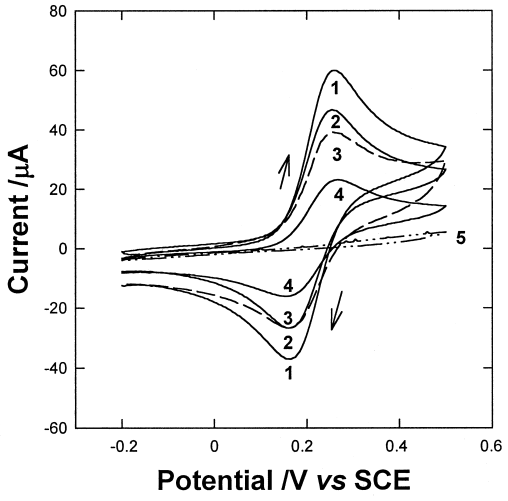

Fig. 9 Cyclic voltammogramms between –0.2 and 0.5 V *vs*. SCE for PQC Au electrodes in 0.20 mol l^{-1} KCl + 2.00 mmol l^{-1} $K_4Fe(CN)_6$ aqueous solution. dE/dt = 20 mV s^{-1}. The solutions were exposed to air. Only curve 5 is for the 1-dodecanethiol-modified Au electrode; the other curves are for the bare gold electrode. Curves 1 and 5: the Au electrodes were submerged in the solution; 2: the Au electrode was partially immersed (R_1 = 210 Ω); 3: the Au electrode was partially immersed (R_1 = 209 Ω), but its R_1 value was achieved after a potential step from the open-circuit potential to –0.8 V *vs*. SCE for 350 s for a partially immersed electrode primarily with R_1 = 100 Ω (curve 4); 4: the Au electrode was partially immersed (R_1 = 100 Ω).

step from the open-circuit potential to –0.8 V *vs*. SCE for 350 s gave peak currents obviously larger than those recorded at this partially immersed Au electrode before the potential step (curve 4, R_1 = 100 Ω), but smaller than those recorded on a partially immersed electrode directly with an R_1 value of 210 Ω (curve 2), indicating that some $K_4Fe(CN)_6$ was present in the solution of lifted meniscus after the potential step, although its concentration was smaller than that in the bulk solution, which can be qualitatively explained by dilution of the water produced after oxygen reduction and that the solution meniscus rising as above was not a direct and net rising of the bulk solution.

However, the above-mentioned electrode product collection mechanism alone encounters difficulties in explaining quantitatively relationships between the electric charge (or the amount of water produced) during oxygen reduction and the raised amplitude of the solution meniscus estimated from the EQCIS responses. For the potential-step EQCIS experiment shown in Fig. 10, the electric charge consumed from 2000 to 7500 s was –0.584 C, corresponding to the production of 54.5 μg or 0.0545 μl water based on the assumption of 100% current efficiency of oxygen reduction reaction ($O_2 + 4H^+ + 4e = 2H_2O$), while ΔH_i = 0.123 cm corresponding to ΔA_i = 0.072 cm^2 was achieved. Therefore, by assuming the 0.0545 μl water could be uniformly distributed at the newly wetted electrode surface of 0.072-cm^2 area (ΔA_i), the thickness of the water was found to be 7.57 μm, which is larger than the characteristic decay length (δ) of the shear oscillation wave for a 9-MHz PQC in water ($\delta = [\eta_L/(\pi\rho_L f_0)]^{1/2} \approx 0.188$ μm),[28] indicating that continued collection of the electrochemical product at the upper edge of the solution meniscus truly played an important role in the rising of solution meniscus observed here on partially immersed Au electrodes. However, the electric charge consumed from 300 to 400 s, –4.46 mC, corresponds to the production of 0.416 μg or 4.16×10^{-4} μl water, while ΔH_i = 0.148 cm, equivalent to ΔA_i = 0.101 cm^2, was achieved, as shown in Fig. 10B. The thickness of the water is thus similarly found to be only 4.12×10^{-2} μm, which is significantly smaller than the ~0.188 μm characteristic decay length, demonstrating that, at the initial stage after the potential step from 0.5 to –0.8 V *vs*. SCE, the continued collection of the water produced by oxygen reduction at the upper edge of solution meniscus is not a predominant factor for the rising of the solution meniscus. A similar conclusion could be drawn from cyclic voltammetric experiments by analyzing the relationships between the electric charge and the increases in the immersed electrode height. We suppose that the rapid rising of the aqueous solution meniscus at the initial stage after a potential step from 0.5 to –0.8 V *vs*. SCE may be, in principle, ascribed to a lowering of contact angle hysteresis (or a change in the contact angle) at the oxygen reduction potentials. The problem of the contact angle hysteresis exists as a very complicated phenomenon for most solid | liquid interfaces, resulting from the surface roughness of the solid, chemical contamination or inhomogeneities in the solid and/or organic contaminants, *e.g*. surfactants or polymers in the liquid phase.[22-25] We have determined the advancing contact angles of the Au electrode surface in air by using 4 μl pure water, 0.20 mol l^{-1} KCl + 1.0 mmol l^{-1} HCl, 0.20 mol l^{-1} KCl and 0.10 mol l^{-1} KCl + 0.10 mol l^{-1} NaOH aqueous solutions (6 repeated measurements for each), respectively. The contact angles were 61 ± 5° for water, 0.20 mol l^{-1} KCl + 1.0 mmol l^{-1} HCl and 0.20 mol l^{-1} KCl, but was 49 ± 4° for 0.10 mol l^{-1} KCl + 0.10 mol l^{-1} NaOH. In addition, after thoroughly stirring the 4 μl solution drop with a microsyringe needle to equilibrate the liquid wetting on the Au electrode surface, the contact angles became smaller, *i.e*. 36 ± 4° were found for water, 0.20 mol l^{-1} KCl + 1.0 mmol l^{-1} HCl and 0.20 mol l^{-1} KCl, and 21 ± 3° for 0.10 mol l^{-1} KCl + 0.10 mol l^{-1} NaOH aqueous solution. Since smaller contact angles were observed for the alkaline solution and the reduction of oxygen at partially immersed Au electrodes was accompanied with a pH increase at

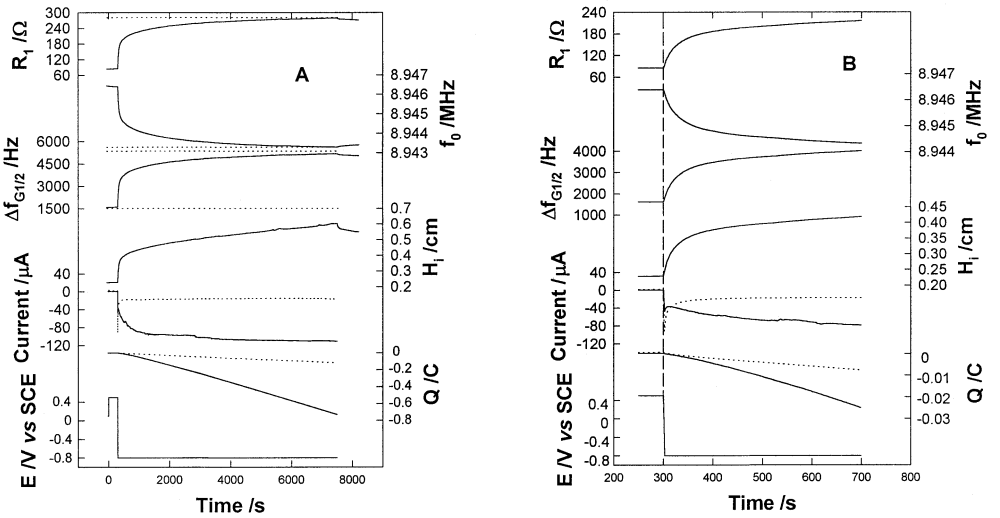

Fig. 10 EQCIS and H_i responses for a PQC Au electrode partially (solid lines) and totally (dashed lines) immersed in 0.20 mol l^{-1} KCl aqueous solution during double potential-step experiments. The potential was first stepped from the open-circuit potential to 0.5 V for 300 s, then stepped to –0.8 V *vs*. SCE for 7200 s. The broken line in Fig. 10B indicates the time when the potential step from 0.5 to –0.8 V *vs*. SCE began. The solution was exposed to air.

the upper edge of solution meniscus, relatively high wetting of the Au electrode after oxygen reduction, *i.e*. the rising of the solution meniscus, could be detected, as shown in the above figures for EQCIS experiments. Furthermore, as shown in Fig. 7, since, before the potential cycling experiment, the Au electrode had been wetted to a greater extent in the alkaline $NaClO_4$ solution, the rising of the solution meniscus during potential cycling should not be so significant as compared with those in acidic and neutral $NaClO_4$ solutions. In addition, polarization at the oxygen reduction potentials may also be effective for removing the oxygen adsorbed previously or other adsorbates immediately, and thus the cleaning of the Au electrode surface can lower the contact angle hysteresis and cause the rising of aqueous solution meniscus, though the amount of adsorbates appeared to be very small and was not detected electrochemically (the pure Au is intrinsically hydrophilic with an advancing contact angle close to 0˚).[29,30] In summary, the rising of the aqueous solution meniscus for partially immersed Au electrodes can be ascribed to a lowering of the contact angle hysteresis (or a change in the contact angle) and continued collection of the water product at the upper edge of the solution meniscus at the oxygen reduction potentials. It should be noted that, as shown in Fig. 10, the turn-off of the –0.8 V *vs*. SCE polarization led to a decrease in H_i, which is probably ascribed to volatilization of the thin water/electrolyte layer at the upper edge of the solution meniscus formed during oxygen reduction. R_1 and H_i could begin their increases again if the –0.8 V potential was re-applied.

Conclusion

In summary, we have investigated the effects of the partial immersion of an Au electrode on the EQCIS responses, and developed a method for the *in situ* determination of the immersed area and height of the PQC electrode. The rising of the aqueous solution meniscus for a gold electrode partially immersed in aqueous solutions was found during oxygen reduction. The meniscus rising has been ascribed to both the reduction of the contact-angle hysteresis (or a change in the contact angle) and the continued collection of the water produced electrochemically at the upper edge of the solution meniscus at oxygen reduction potentials. It should be noted that the density and viscosity of the solution in the lifted solution meniscus moieties may differ to a certain extent from those of the bulk solution, and this difference is not easy to be evaluated and corrected *in situ*; therefore, the estimation of H_i and A_i during the potential-cycling and potential-step experiments based on Eq. (5) for each corresponding electrolyte solution should have some errors. However, since, for example, R_1 changed by only ~8 Ω from 0.20 mol l^{-1} to 2.0 mmol l^{-1} $NaClO_4$ (or KCl) aqueous solution, *i.e*. ~3% of the R_1 change from air to the 0.20 mol l^{-1} $NaClO_4$ (or KCl) aqueous solution, we believe that the relative errors for H_i and A_i estimations by the present EQCIS technique may generally be smaller than ~3%, besides its obvious advantage capable of *in situ* measurements of H_i and A_i in electrochemical processes.

Acknowledgements

This work was supported by the National Natural Science Foundation of China, the Teaching and Research Award Program for Outstanding Young Teachers in Higher Education Institutions of MOE, P. R. C., the Science and Technology Foundation of Hunan Province for Young Scientists and the Natural Science Foundation of Hunan Province.

References

1. D. A. Buttry, in "*Electroanalytical Chemistry*", ed. A. J. Bard, **1991**, Vol. 17, Marcel Dekker, New York, 1.
2. M. A. Noël and P. A. Topart, *Anal. Chem.*, **1994**, *66*, 484.
3. M. A. Noël and P. A. Topart, *Anal. Chem.*, **1994**, *66*, 2926.
4. H. L. Bandey, M. Gonsalves, A. R. Hillman, A. Glidle, and S. Bruckenstein, *J. Electroanal. Chem.*, **1996**, *410*, 219.
5. M. Skompska and A. R. Hillman, *J. Chem. Soc. Faraday*

Trans., **1996**, *92*, 4101.
6. R. Etchenique and E. J. Calvo, *Anal*. *Chem*., **1997**, *69*, 4833.
7. Q. Xie, H. Liu, Y. Zhang, and S. Yao, *Chin*. *J*. *Chem*., **1999**, *17*, 491.
8. Q. Xie, Y. Zhang, Y. Yuan, Y. Guo, X. Wang, and S. Yao, *J*. *Electroanal*. *Chem*., **2000**, *484*, 41.
9. Q. Xie, J. Wang, A. Zhou, Y. Zhang, H. Liu, Z. Xu, Y. Yuan, M. Deng, and S. Yao, *Anal*. *Chem*., **1999**, *71*, 4649.
10. Q. Xie, Y. Zhang, M. Xu, Z. Li, Y. Yuan, and S. Yao, *J*. *Electroanal*. *Chem*., **1999**, *478*, 1.
11. S. J. Martin, V. E. Granstaff, and G. C. Frye, *Anal*. *Chem*., **1991**, *63*, 2272.
12. H. Muramatsu, E. Tamiya, and I. Karube, *Anal*. *Chem*., **1988**, *60*, 2142.
13. F. G. Will, *J*. *Electrochem*. *Soc*., **1963**, *110*, 145.
14. F. G. Will, *J*. *Electrochem*. *Soc*., **1963**, *110*, 152.
15. H. C. Weber, H. P. Meissner, and D. A. Sama, Abstract No. 21, Battery Division, Electrochemical Society, Fall Meeting, Detroit, October, **1961**.
16. A. J. Bard and L. R. Faulkner, "*Electrochemical Methods: Fundamentals and Applications"*, **1980**, John Wiley & Sons, New York.
17. P. Bernabeu, L. Tamisier, and A. De Cesare, *Electrochim*. *Acta*, **1988**, *33*, 1129.
18. T. Zhou, L. Nie, and S. Yao, *J*. *Electroanal*. *Chem*., **1990**, *293*, 1.
19. E. J. Calvo, C. Danilowicz, and R. J. Etchenique, *J*. *Chem*. *Soc*. *Faraday Trans*., **1995**, *91*, 4083.
20. M. D. Ward and E. J. Delawski, *Anal*. *Chem*., **1991**, *63*, 886.
21. A. C. Hillier and M. D. Ward, *Anal*. *Chem*., **1992**, *64*, 2539.
22. P. G. De Gennes, *Revs*. *Mod*. *Phys*., **1985**, *57*, 827.
23. L. S. Penn and B. J. Miller, *Colloid Interface Sci*., **1980**, *77*, 574.
24. R. J. Good, in "*Surface and Colloid Science*", ed. R. J. Good and R. R. Stromberg, **1979**, Vol. 11, Plennum, New York.
25. M. G. Nicholas and R. M. Crispin, *J*. *Mater*. *Sci*., **1986**, *21*, 522.
26. J. O'M. Bockris, S. D. Argade, and E. Gileadi, *Electrochim*. *Acta*., **1969**, *14*, 1259.
27. I. Morcos, *J*. *Colloid Interface Sci*., **1971**, *37*, 410.
28. K. K. Kanazawa and J. G. Gordon II, *Anal*. *Chim*. *Acta*., **1985**, *175*, 99.
29. R. D. Vold and M. J. Vold, in "*Colloid and Interface Chemistry*", **1983**, Addison-Wesley, London.
30. A. W. Adamson, "*Physical Chemistry of Surfaces*", **1982**, Wiley, New York.